Supporting Information

Accurately controlling the hierarchical nanostructure of polyamide membrane *via* electrostatic atomization-assisted interfacial polymerization

Jingjing Chen[a,1], Jie Zhang[a,1], Xiaoli Wu[a], Xulin Cui[a], Wenpeng Li[a,*], Haoqin Zhang[a], Jingtao Wang[a,b,*] Xingzhong Cao[c], Peng Zhang[c]

[a]School of Chemical Engineering, Zhengzhou University, Zhengzhou 450001, P. R. China

[b]Henan Institutes of Advanced Technology, Zhengzhou University, 97 Wenhua Road, Zhengzhou 450003, P. R. China

[c]Multi-discipline Research Division, Institute of High Energy Physics, Chinese Academy of Sciences, Beijing 100049, P. R. China

*To whom correspondence should be addressed: E-mail: lwp0103@163.com (W.P. Li); jingtaowang@zzu.edu.cn (J.T. Wang).

[1]These authors contributed equally to this work.

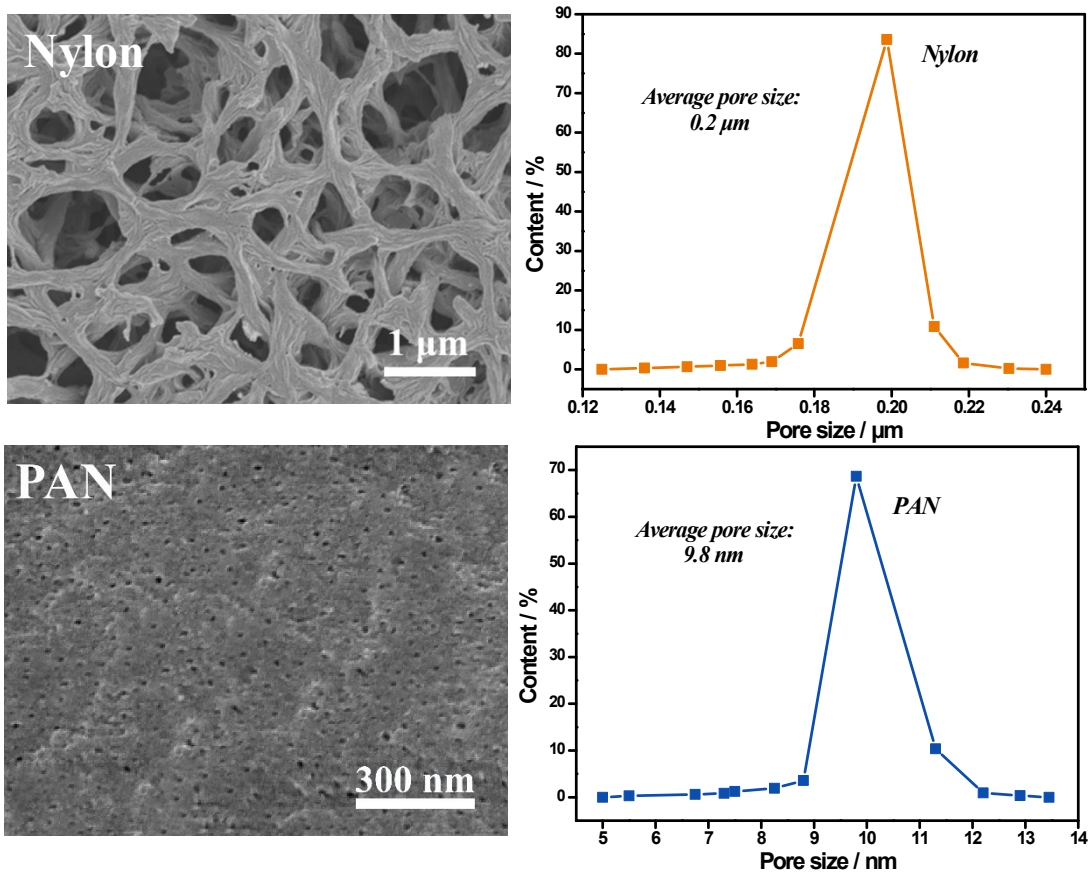

Fig. S1. SEM images of nylon and PAN substrates and the corresponding pore size distribution.

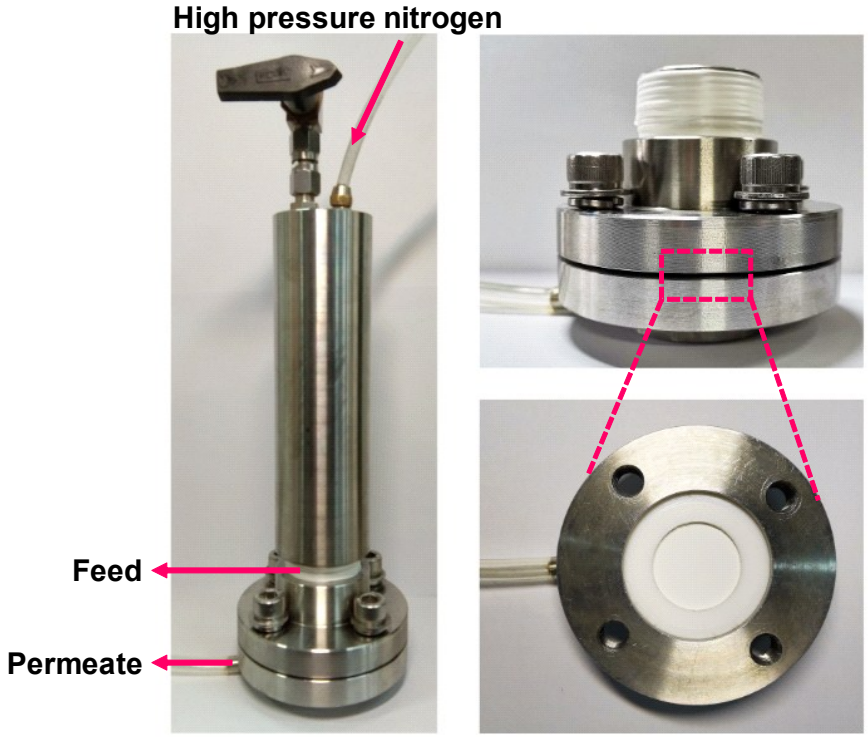

Fig. S2. The home-made device for the nanofiltration performance evaluation of membranes.

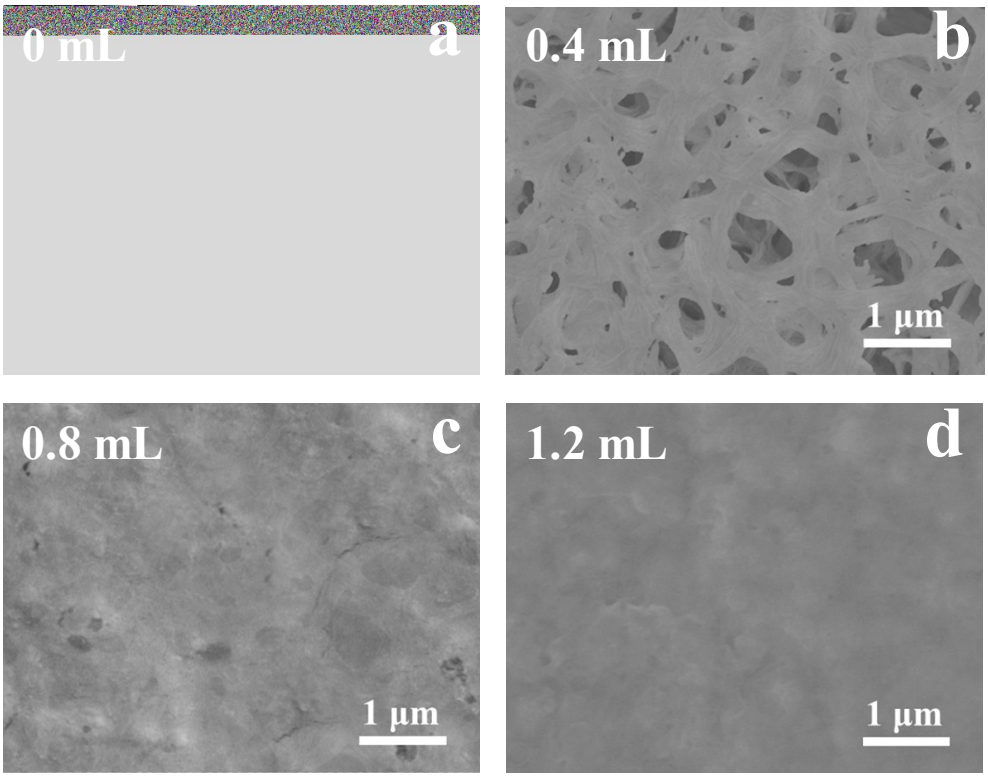

Fig. S3. SEM images of $TMC_{0.001}$ membrane with different monomer amounts.

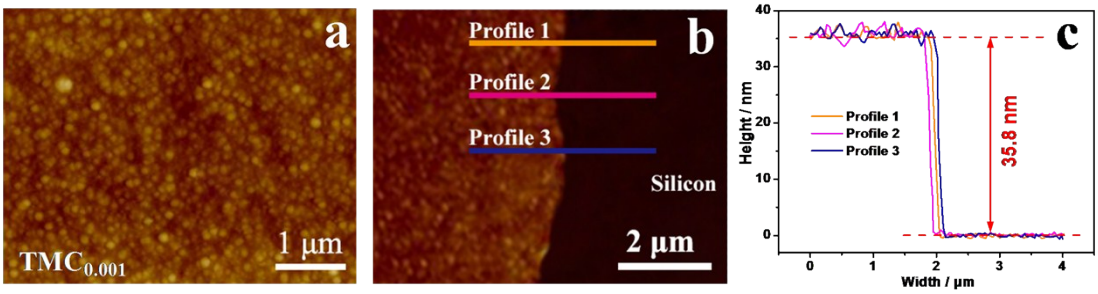

Fig. S4. (a) AFM image of $TMC_{0.001}$ membrane on nylon substrate, (b) AFM height image and (c) corresponding height profiles of $TMC_{0.001}$ membrane with same monomer amounts on silicon wafer.

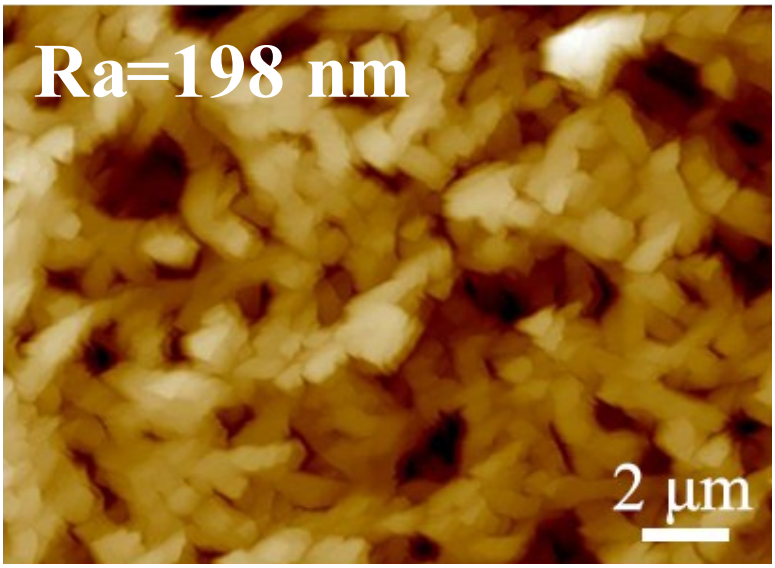

Fig. S5. AFM image of nylon substrate.

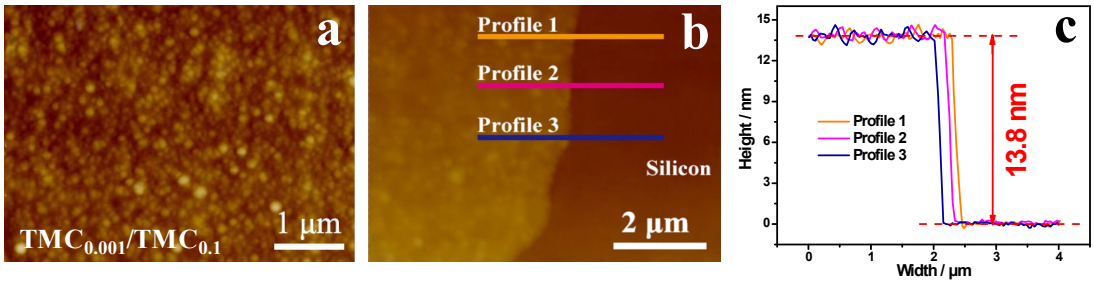

Fig. S6. (a) AFM image of $TMC_{0.001}/TMC_{0.1}$ membrane on nylon substrate, (b) AFM height image and (c) corresponding height profiles of $TMC_{0.1}$ membrane with same monomer amounts as the dense layer in $TMC_{0.001}/TMC_{0.1}$ on silicon wafer.

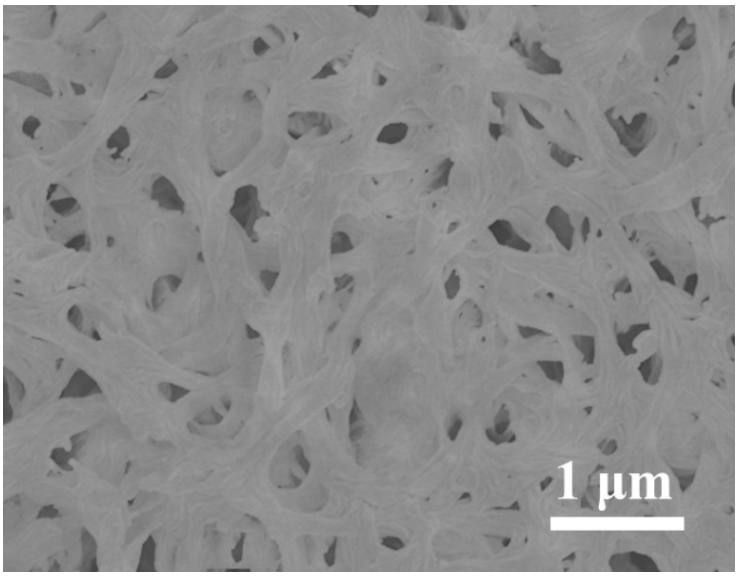

Fig. S7. SEM image of $TMC_{0.1}$ membrane with same monomer amounts as the dense layer in $TMC_{0.001}/TMC_{0.1}$ directly prepared on nylon substrate.

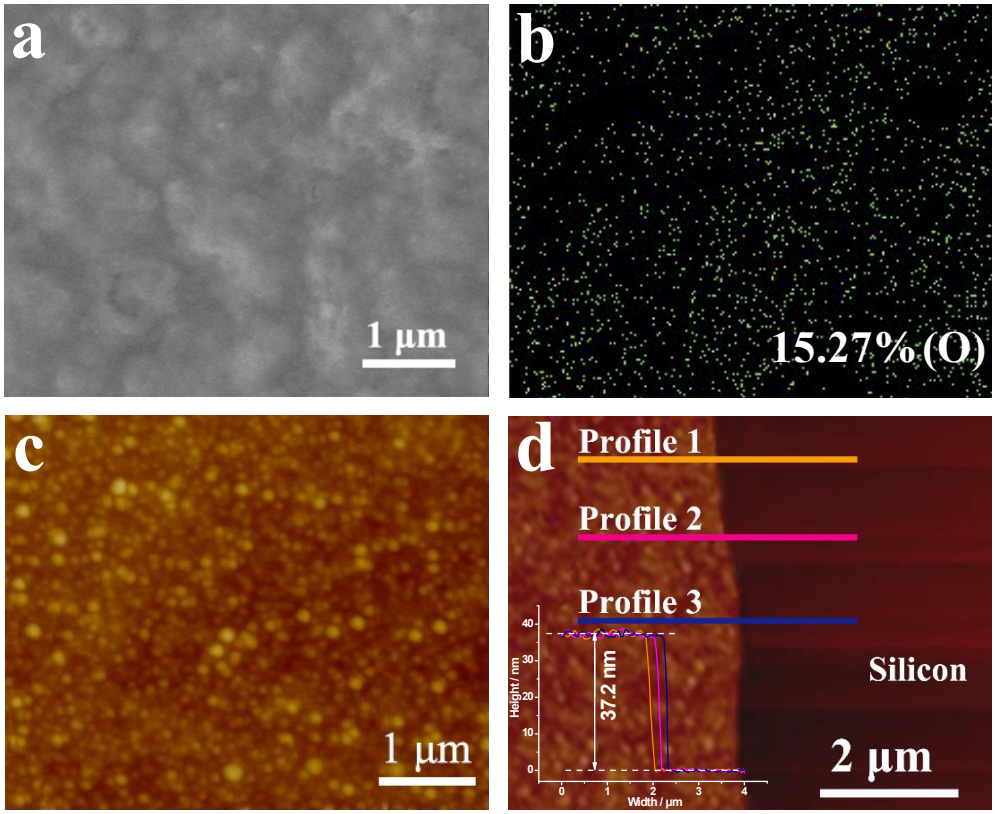

Fig. S8. (a) SEM image, (b) O elemental mapping, and (c) AFM image of defect-free $TMC_{0.1}$ membrane. (d) AFM height image of $TMC_{0.1}$ membrane with the same monomer amount but on silicon wafer (Inset is the corresponding height profiles).

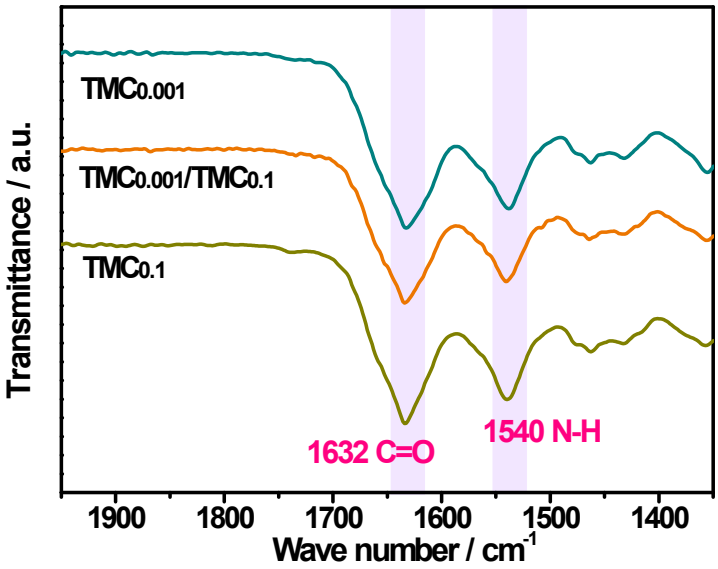

Fig. S9. FTIR spectra of $TMC_{0.001}$, $TMC_{0.001}/TMC_{0.1}$, and $TMC_{0.1}$ membranes.

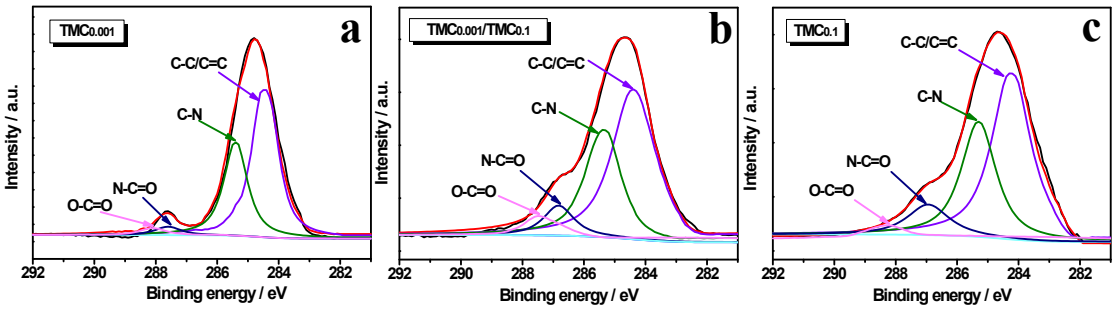

Fig. S10. High resolution C 1s spectra of $TMC_{0.001}$, $TMC_{0.001}/TMC_{0.1}$, and $TMC_{0.1}$ membranes.

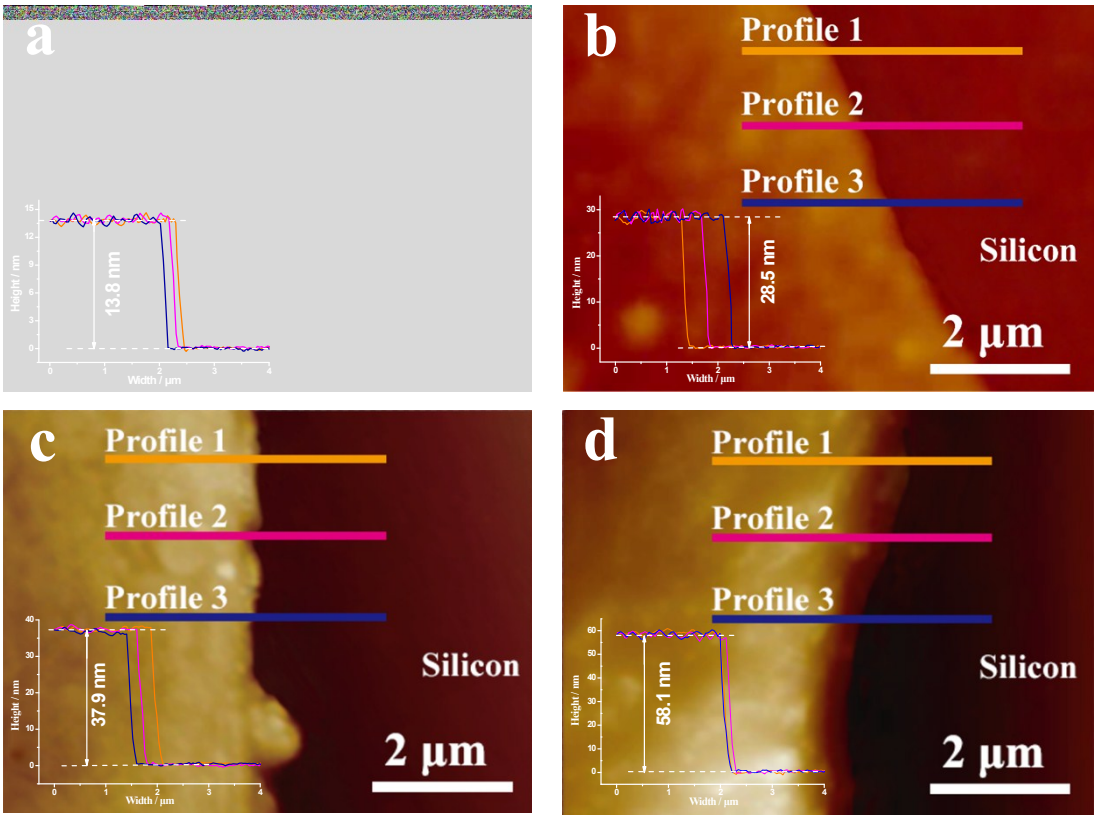

Fig. S11. AFM images of $TMC_{0.1}$ membranes at (a) 0.4 ml, (b) 0.8 ml, (c) 1.2 ml, and (d) 1.6 ml monomer solutions (Insets are corresponding height profiles).

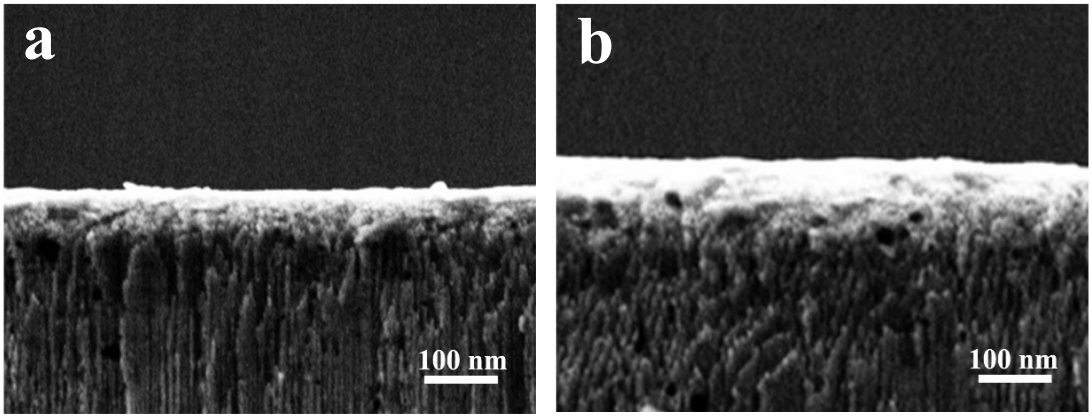

Fig. S12. Cross-sectional SEM images of $TMC_{0.1}$ membrane sprayed for (a) 5 h and (b) 10 h.

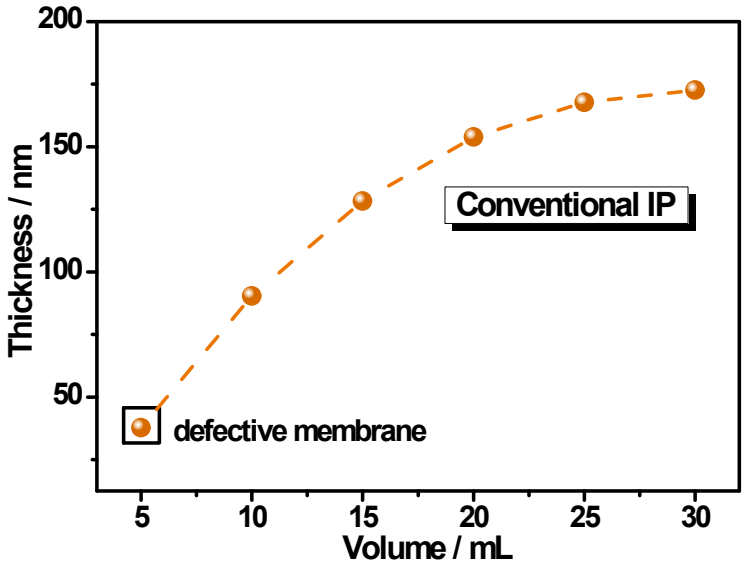

Fig. S13. Thickness of conventional IP membranes as a functional of monomer amounts.

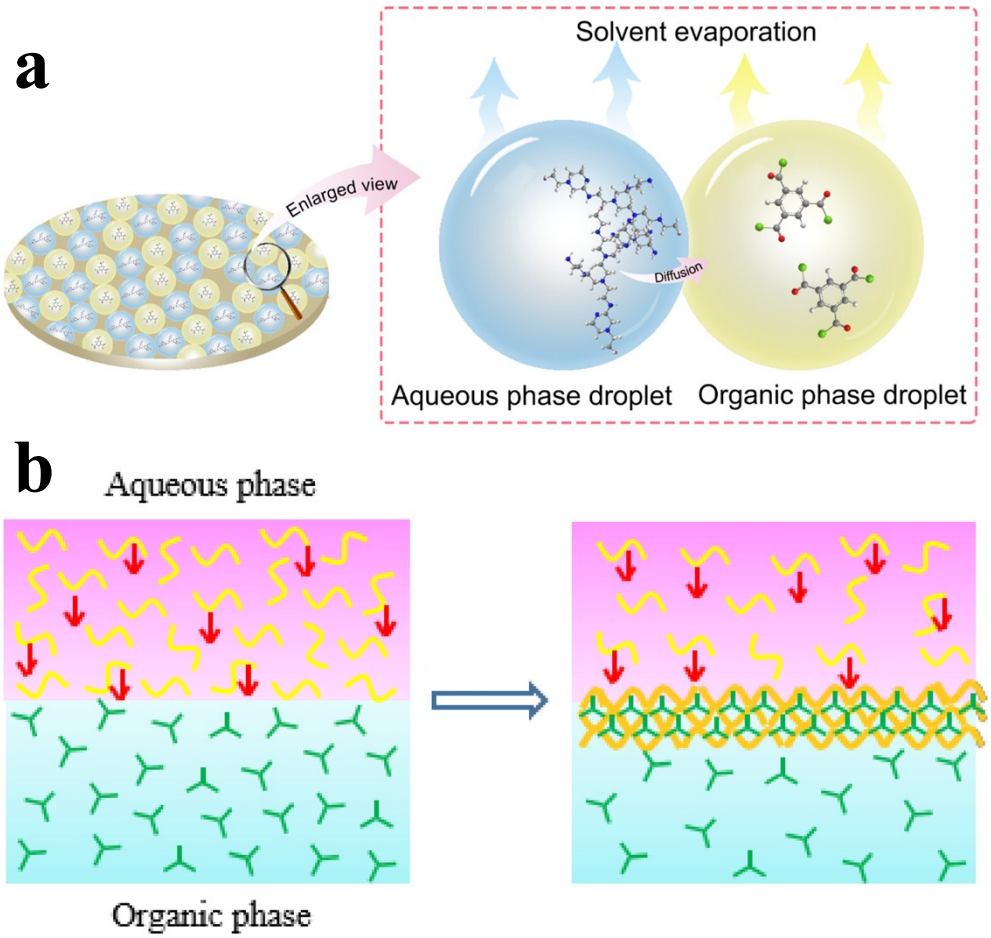

Fig. S14. The comparison of schematic diagram between (a) electrostatic atomization-assisted and (b) conventional interfacial polymerization[1].

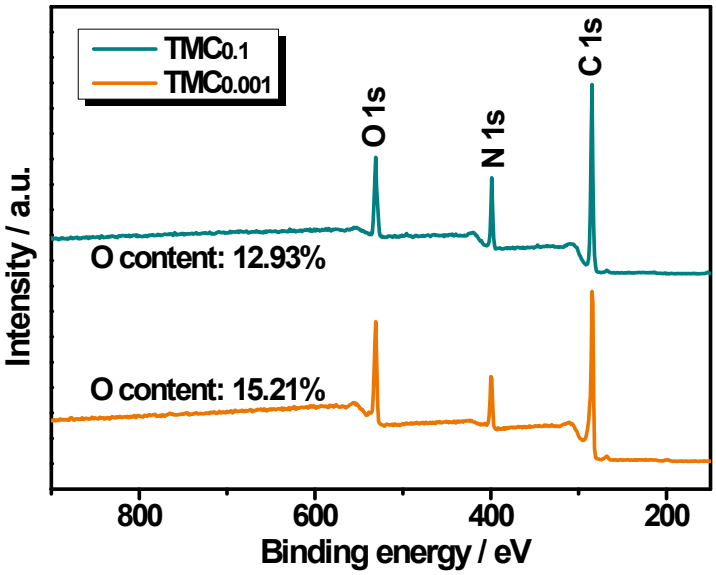

Fig. S15. XPS spectra of the $TMC_{0.1}$ and $TMC_{0.001}$ membranes whose aqueous phase monomer is *p*-phenylenediamine (PPD).

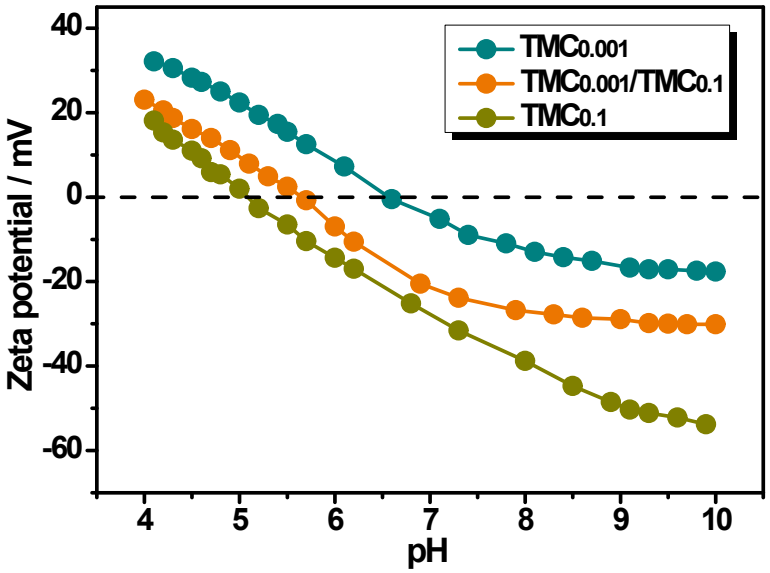

Fig. S16. Zeta potential of $TMC_{0.001}$, $TMC_{0.001}/TMC_{0.1}$, and $TMC_{0.1}$ membranes at different pH.

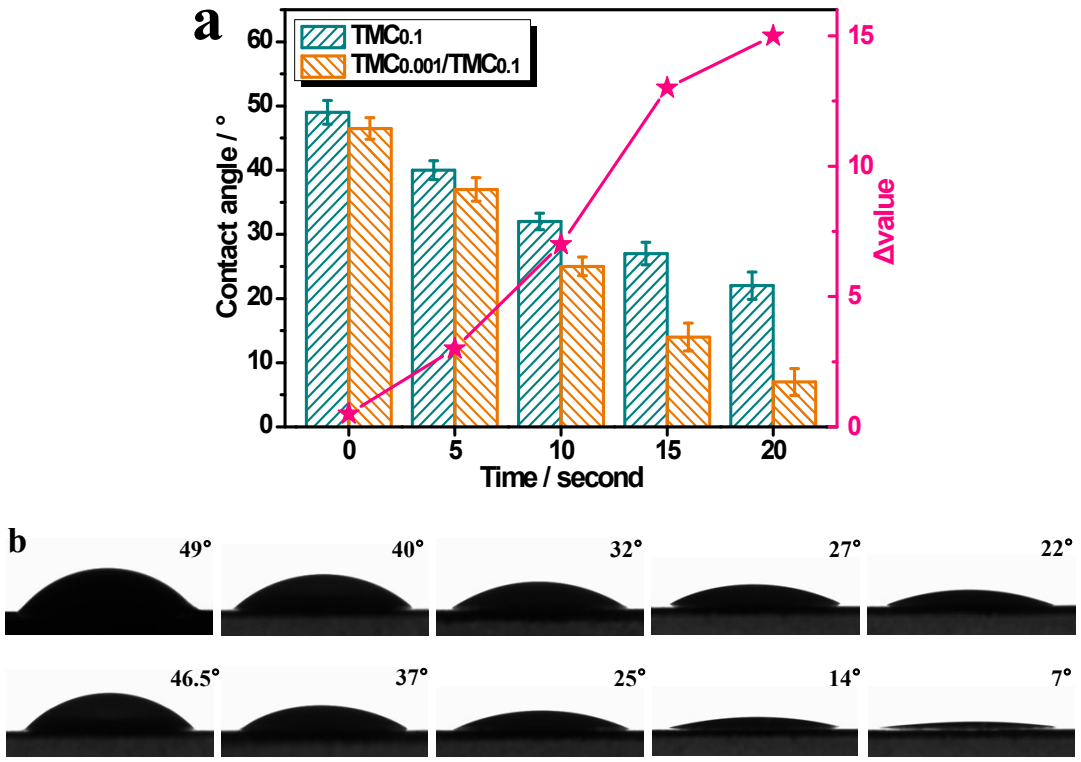

Fig. S17. (a) Contact angles of $TMC_{0.1}$ and $TMC_{0.001}/TMC_{0.1}$ membranes as well as (b) the corresponding photos.

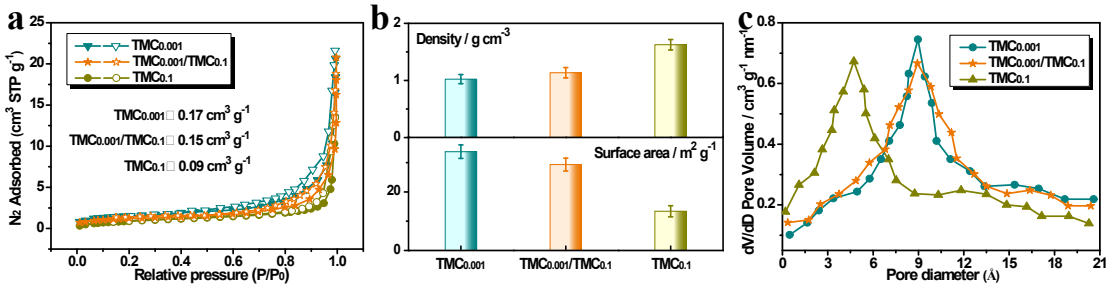

Fig. S18. (a) N_2 adsorption/desorption isotherms, (b) calculated surface area and density, and (c) pore diameter distribution of $TMC_{0.001}$, $TMC_{0.001}/TMC_{0.1}$, and $TMC_{0.1}$ membranes.

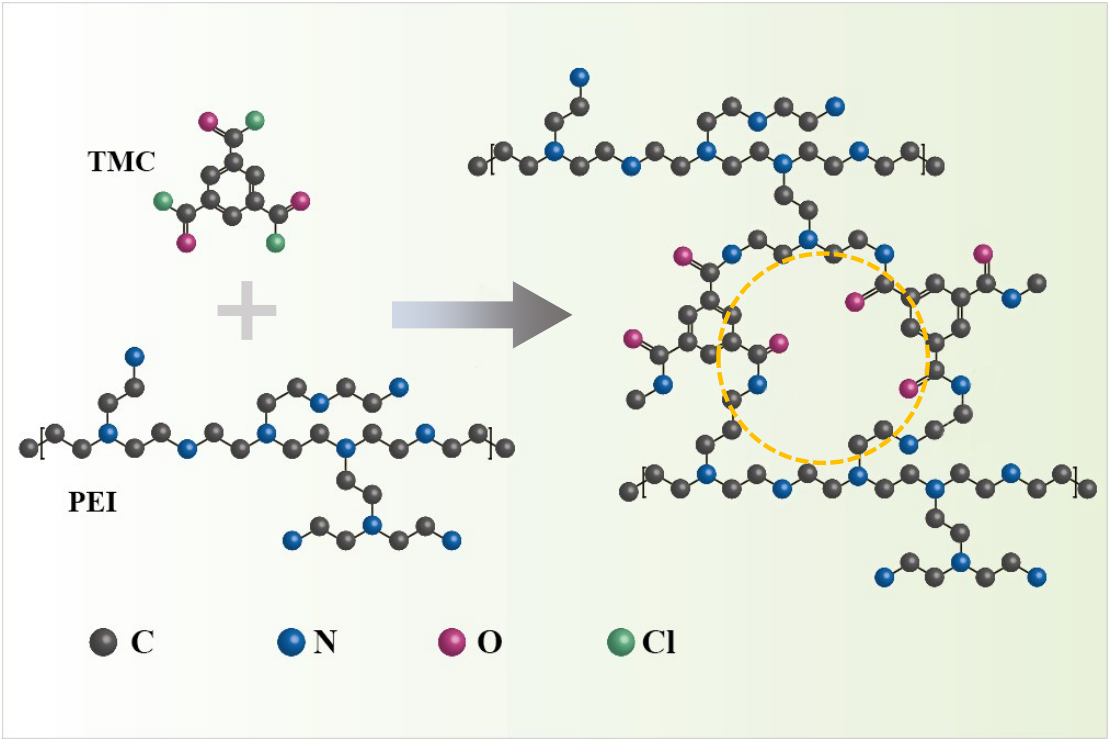

Fig. 19. The reaction diagram of PEI and TMC as well as the formed nanopore.

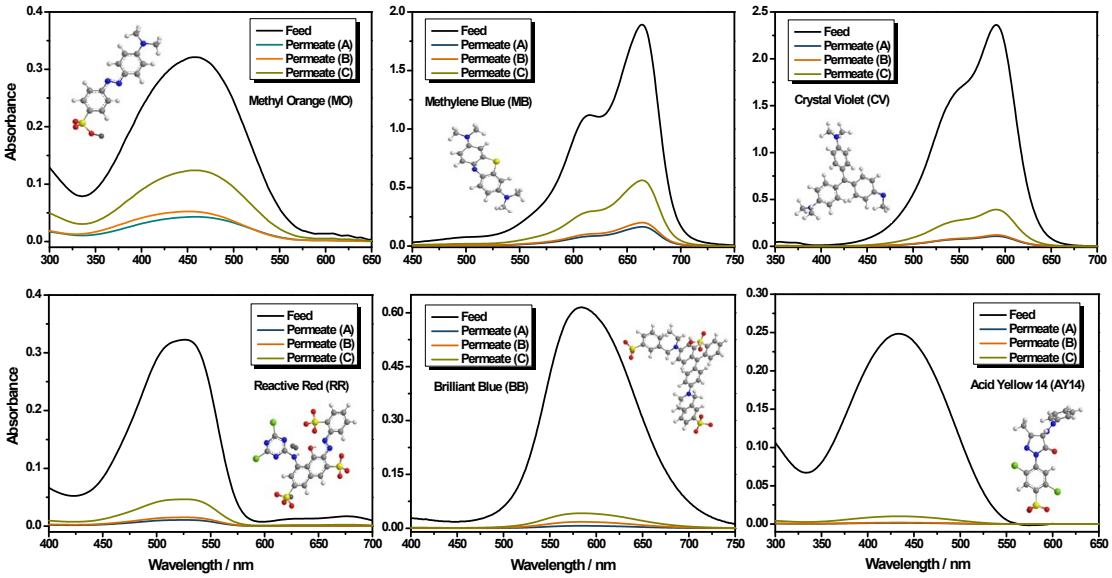

Fig. S20. UV-vis spectra of dyes with different sizes in methanol solution before and after filtration through (A) $TMC_{0.001}$, (B) $TMC_{0.001}/TMC_{0.1}$, and (C) $TMC_{0.1}$ membranes.

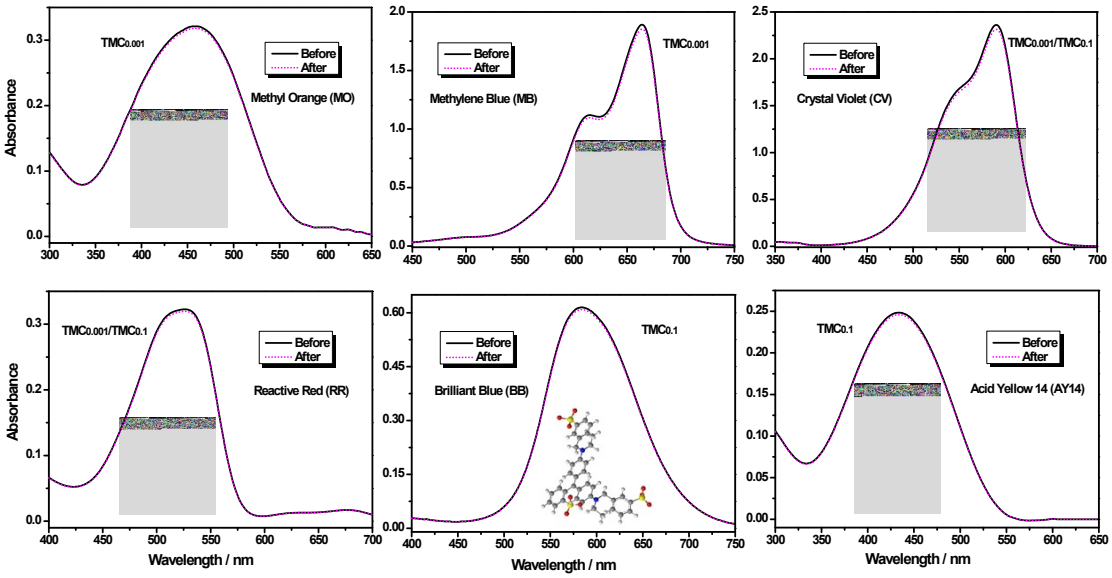

Fig. S21. UV-vis absorption spectra of dye solutions before and after membrane immersion for 3 hours.

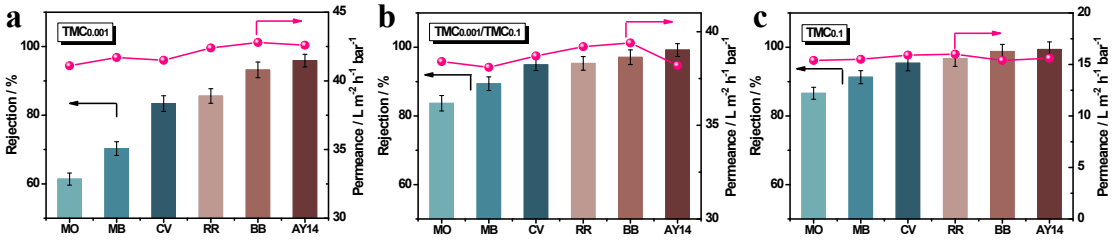

Fig. S22. Dyes rejection and methanol permeance of (a) $TMC_{0.001}$, (b) $TMC_{0.001}/TMC_{0.1}$, and (c) $TMC_{0.1}$ membranes.

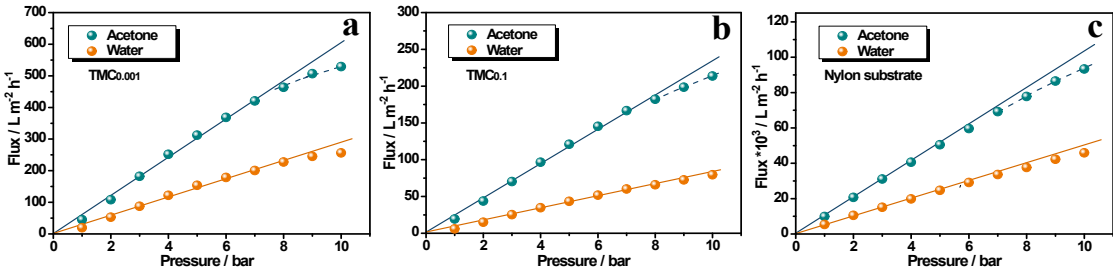

Fig. S23. Acetone and water fluxes of (a) $TMC_{0.001}$ and (b) $TMC_{0.1}$ membranes as well as (c) nylon substrate as a function of operation pressure.

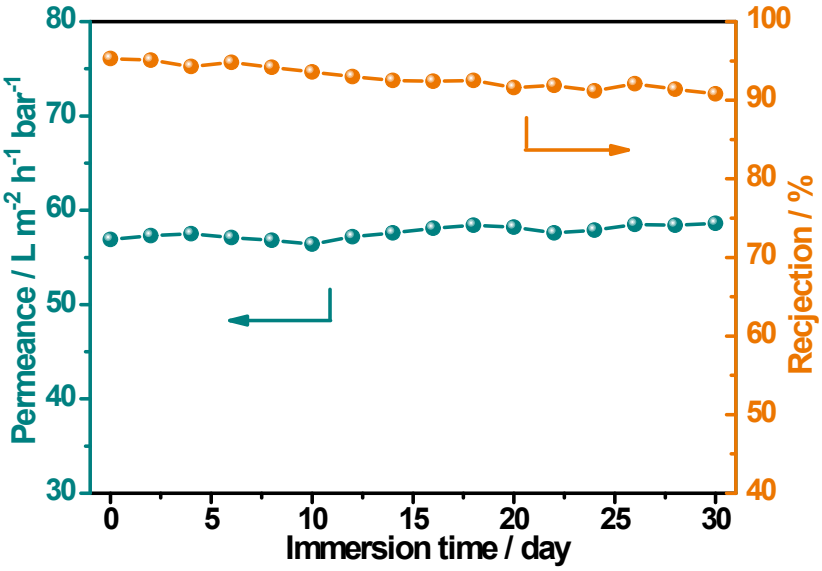

Fig. S24. Long-term water stability of $TMC_{0.001}/TMC_{0.1}$ membrane (pH=4.0).

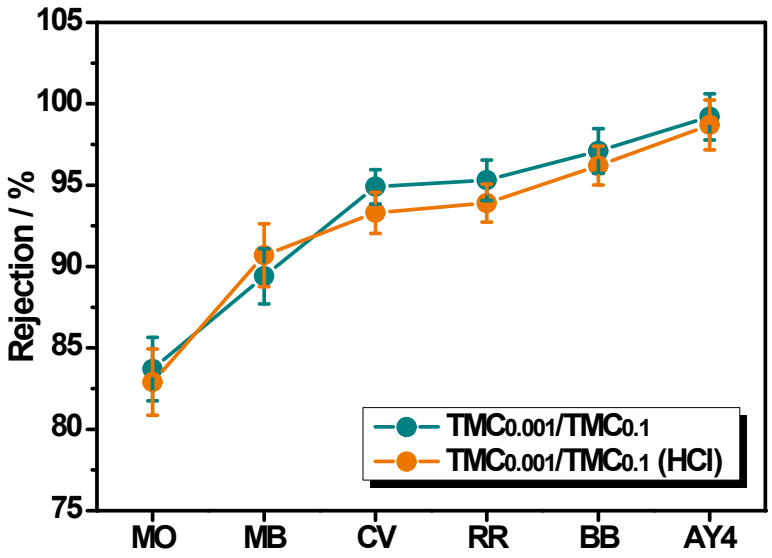

Fig. S25. Rejection of $TMC_{0.001}/TMC_{0.1}$ membrane before and after HCl treatment for one month.

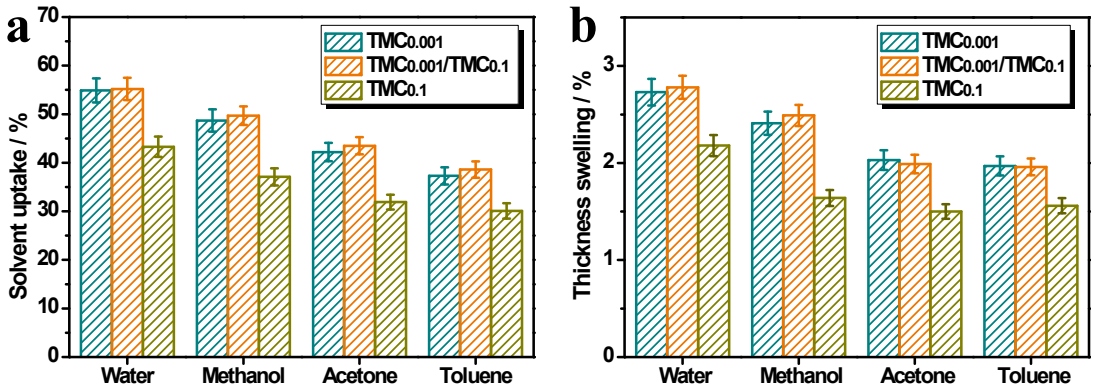

Fig. S26. (a) Solvent uptake and (b) thickness swelling of $TMC_{0.001}$, $TMC_{0.001}/TMC_{0.1}$, and $TMC_{0.1}$ membranes.

Table S1. Elemental composition of $TMC_{0.1}$ and $TMC_{0.001}$ membranes formed from PPD was detected by XPS.

Membrane	Aqueous phase (w/v)	Organic phase (w/v)	Elemental composition (%)			Cross-linking degree (%)
			C	O	N	
$TMC_{0.1}$	0.1%	0.1%	74.63	12.93	12.44	94.1
$TMC_{0.001}$	0.1%	0.001%	72.14	15.21	11.32	56.4

Table S2. Dyes properties and nanofiltration performance of $TMC_{0.001}$/$TMC_{0.1}$ membrane.

Dye molecular	Size (nm)	Charge	Methanol permeance (L m^{-2} h^{-1} bar^{-1})	Rejection (%)
MO	1.0	−	38.4	87.3
MB	1.2	+	38.1	89.4
CV	1.5	+	38.7	94.9
RR	1.5	−	39.2	95.3
BB	1.6	−	39.4	97.1
AY14	1.9	−	38.2	99.2

Table S3. Comparison of nanofiltration performance for various membranes.

Membrane	Thickness of skin layer (nm)	Solute	Rejection (%)	Water permeance (L m^{-2} h^{-1} bar^{-1})	Reference
TFCn	54.9	Methyl orange	90	19.6	2
MDC-IP	25	Acid fuchsin	98.5	13.8	3
PIP-TMC	43.6	Reactive orange	95	7.11	4
TPT-TMC	35.1	Reactive orange	97	8.68	4
TA/DETA	57	Chrysoidine G	98	7.9	5
PIP-GO	20	Rhodamine B	87	24.2	6
NFM-4	98	Safranine T	95	9.82	7
SRNF	93	Congo red	99.9	2.7	8
NFM-6	77	Methyl orange	95	17.6	9
PAN450	35	Methyl blue	96	5.8	10
SPIF-PA	17.1	Acid fuchsin	99	0.86	11
IP@FI	6.5	Neutral red	96	2.7	12
E-spray	30	Methyl orange	91	2	13
$TMC_{0.001}/TMC_{0.1}$	49.6	Acid yellow 14	99.2	23.7	This work

Supplementary References

1. L. Shan, J. Gu, H. Fan, S. Ji and G. Zhang, *ACS Appl. Mater. Interfaces*, 2017, **9**, 44820−44827.
2. Y. Li, Y. Su, Y. Dong, X. Zhao, Z. Jiang, R. Zhang and J, Zhao, *Desalination*, 2014, **333**, 59–65.
3. L Shan, J. Gu, H. Fan, S. Ji and G. Zhang, *ACS Appl. Mater. Interfaces*, 2017, **9**, 44820–44827.
4. Y. Zeng, L. Wang, L. Zhang and J. Q. Yu, *J. Membr. Sci.*, 2018, **546**, 225–233.
5. X. Zhang, Y. Lv, H. Yang, Y. Du and Z. Xu, *ACS Appl. Mater. Interfaces*, 2016, **8**, 32512–32519.
6. R. Hu, Y. He, C. Zhang, R. Zhang, J. Li and H. Zhu, *J. Mater. Chem. A*, 2017, **5**, 25632–25640.
7. Q. An, W. Sun, Q. Zhao, Y. Ji and C. Gao, *J. Membr. Sci.*, 2013, **431**, 171–179.
8. S. Hermans, E. Dom, H. Mariën, G. Koeckelberghs and I. F. J. Vankelecom, *J. Membr. Sci.*, 2015, **476**, 356–363.
9. Y. Mi, F. Zhao, Y. Guo, X. Weng, C. C. Ye and Q. An, *J. Membr. Sci.*, 2017, **541**, 29–38.
10. M. R. Chowdhury, J. Steffes, B. D. Huey and J. R. McCutcheon, *Science*, 2018, **361**, 682–686.
11. M. F. J. Solomon, Y. Bhole and A. G. Livingston, *J. Membr. Sci.*, 2012, **423**, 371–382.
12. Z. Jiang, S. Karan and A. G. Livingston, *Adv. Mater.*, 2018, **30**, 1705973.
13. X. Ma, Z. Yang, Z. Yao, H. Guo, Z. Xu and C. Y. Tang, *Environ. Sci. Technol. Lett.*, 2018, **5**, 117–122.